

# Study of different reference axes for secondary vertexing in DIS at ZEUS

Jannik Hofestädt

14th July - 3rd September 2010

Supervisor: Achim Geiser

**Abstract:** This report describes my project during the DESY Summer Student Program 2010. I studied different reference axes for secondary vertexing in deep inelastic scattering at the ZEUS detector at HERA. These axes were jets with different transverse energy, pseudo-thrust axes and the axis of the hadronic system. A combined method of the former two axes improves the measurement most.

## Contents

<b>1. Introduction</b>	<b>3</b>
<b>2. Heavy Flavor Physics at HERA</b>	<b>3</b>
2.1. Beauty and charm pair production at HERA . . . . .	3
2.2. Heavy flavor tagging . . . . .	3
<b>3. Monte-Carlo samples</b>	<b>4</b>
<b>4. Event selection</b>	<b>4</b>
<b>5. Reconstruction of secondary vertices</b>	<b>4</b>
<b>6. Secondary vertices from jets as reference axes</b>	<b>5</b>
6.1. Jet selection . . . . .	5
6.2. Significance distributions from high $E_T$ jets . . . . .	5
6.3. Comparison between high $E_T$ jets and all jets . . . . .	6
<b>7. Secondary vertices from Pseudo Thrust axes as reference axes</b>	<b>6</b>
7.1. Pseudo Thrust . . . . .	7
7.2. Implementation of the pseudo thrust axes . . . . .	8
7.3. Pseudo thrust cuts . . . . .	8
7.4. Comparison between high $E_T$ jets and pseudo thrust axes . . . . .	8
7.5. Comparison between the direction of the pseudo thrust and the nearest jet . .	9
7.6. Comparison between projecting onto jets and onto pseudo thrust axes . . . . .	10
<b>8. Secondary vertices from a combined method of jets and pseudo thrust axes</b>	<b>11</b>
8.1. Comparison between combined method and the single methods . . . . .	11
<b>9. The axis of the hadronic system for secondary vertices</b>	<b>12</b>
<b>10. Summary and Outlook</b>	<b>13</b>
<b>11. Acknowledgements</b>	<b>13</b>
<b>Appendix</b>	<b>14</b>
<b>A. Applied Cuts</b>	<b>14</b>
A.1. Event selection cuts . . . . .	14
A.2. Jet selection cuts . . . . .	15
A.2.1. Tracks for secondary vertexing selection cuts . . . . .	15
A.2.2. Secondary vertex from jets selection cuts . . . . .	15
A.3. Pseudo thrust selection cuts . . . . .	15
A.3.1. Secondary vertex from pseudo thrust selection cuts . . . . .	15

## 1. Introduction

The proton ( $p$ ) is not a fundamental particle like the electron ( $e$ ). In the quark parton model the former is composed of three valence quarks: two up quarks and one down quark. One can study the proton structure in  $ep$ -collisions. This was done at the HERA accelerator, which was operated at DESY from 1992 until June 2007. Around one of the interaction points the ZEUS detector was located.

Although HERA was decommissioned three years ago the recorded data is still being analysed. In one of these analyses [1] and references in this thesis the charm ( $c$ ) and beauty ( $b$ ) production cross sections in deep inelastic scattering (DIS) events are measured. The results from this measurement can be used to test the theoretical predictions of QCD. Furthermore, from this measurement the contribution of charm and beauty production to the structure function  $F_2$  can be obtained. These results are also relevant for the Higgs ( $H$ ) searches at LHC, since  $b\bar{b} \rightarrow H$  is one of the possible production mechanisms.

The aim of my Summer Student project was to enhance the statistics and to extend the kinematic range available for the measurement of  $c$  and  $b$  production from inclusive secondary vertices in deep inelastic scattering (DIS). For this goal I studied the extension of the transverse energy ( $E_T$ ) range for jets and new reference axes like the Pseudo-Thrust axes and the axis of the hadronic system for secondary vertices at ZEUS.

## 2. Heavy Flavor Physics at HERA

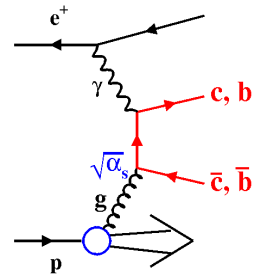
Since 1998 the accelerated electrons or positrons at HERA have an energy of  $27.5\text{ GeV}$  and the protons an energy of  $920\text{ GeV}$ . Therefore, the center-of-mass energy is approximately  $318\text{ GeV}$  and consequently high enough to produce heavy quark pairs ( $b\bar{b}$  or  $c\bar{c}$ ).

Electron-proton scattering events are characterized by the following Lorentz-invariant kinematic variables: the *photon virtuality*  $Q^2$  (negative square of the four-momentum transfer of the exchanged boson), the center-of-mass energy  $\sqrt{s}$ , the Björken scaling variable  $x$  (represents the fraction of momentum of the incoming proton that is carried by the interacting parton in the quark parton model) and the *inelasticity*  $y$ . The meaning of each variable is described in every Particle Physics textbook like [2].

For  $Q^2 \gtrsim 1\text{ GeV}^2$  the  $ep$  events are referred to as deep inelastic scattering (DIS).

### 2.1. Beauty and charm pair production at HERA

The dominant production mechanism for heavy quarks pairs is boson-gluon fusion. In this process, a neutral vector boson, i.e. a photon ( $\gamma$ ) or a  $Z$ , emitted from the incoming electron interacts with a gluon from the proton producing a heavy flavor quark pair. This process is illustrated in the figure on the right hand side.



### 2.2. Heavy flavor tagging

Various experimental techniques are used to tag heavy flavors. Most of them only reconstruct specific final states. For example, beauty production in DIS at HERA has been measured in events with muons and jets by the ZEUS and H1 collaboration [3, 4]. If no decay channel is specified, it is still possible to identify heavy flavor hadrons due to their long lifetime

## 5. Reconstruction of secondary vertices

( $B^0$ :  $c\tau \approx 460 \mu m$  and  $D^0$ :  $c\tau \approx 120 \mu m$  [5]). These long-lived particles can decay after a measurable distance in the detector. To detect these so called *secondary vertices* in the immediate vicinity of the interaction point, the Micro Vertex Detector (MVD) was installed in the ZEUS detector during the shutdown in 2000-2002.

Since the reconstruction of these secondary vertices is crucial for my Summer Student project, it is explained in detail in section 5.

In this analysis, beauty and charm production were studied using inclusive secondary vertices associated to jets and Pseudo-Thrust axes.

## 3. Monte-Carlo samples

For the studies described in this note the Monte-Carlo (MC) samples from the Common Ntuples (v04b) have been used. The studied MC samples were generated for the 06/07p detector configuration. The samples were generated by Rapgap for charm ( $\approx 3.5 \times$  data) and beauty ( $\approx 18 \times$  data).

## 4. Event selection

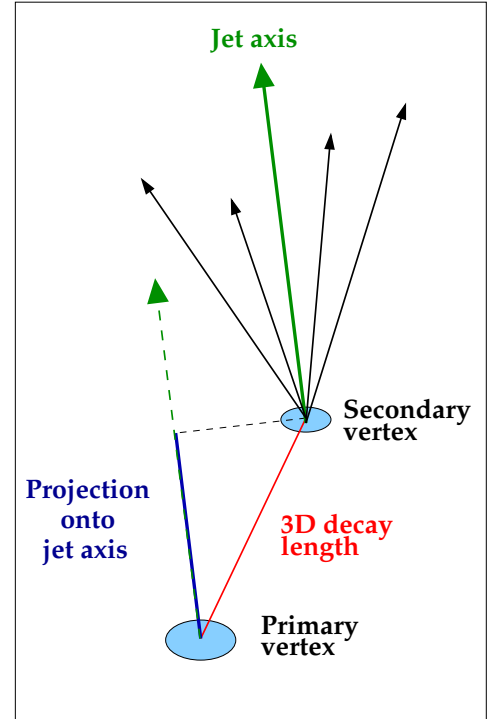
To study the contribution of charm and beauty production to the structure function  $F_2$ , one has to measure the production cross-section as a function of  $x$  and  $Q^2$ . To select DIS events in the range  $5 GeV^2 < Q^2 < 1000 GeV^2$  and  $0.02 < y < 0.7$ , standard cuts like in [1] were applied. A summary of these cuts can be found in the appendix in section A.1.

## 5. Reconstruction of secondary vertices

A reconstructed secondary vertex is always associated to a reference axis. In most cases a jet is used as reference axis, but also other reference axis like the Pseudo Thrust (7.1) are possible.

The case that a secondary vertex associated to a jet was found is illustrated in the right figure [6]. The fit for finding a secondary vertex is performed in 3D. In this study the decay length, which is defined as the distance between the primary interaction vertex (beamspot) and the secondary vertex, is calculated in the  $X$ - $Y$  plane and projected onto the direction of the reference axis. Consequently also negative decay lengths are possible. In the following, the decay length calculated by this procedure is called  $L_{XY}$ .

This procedure is reasonable since the  $Z$ -coordinate of the vertices is not very precise. And it can be assumed that the heavy quark and the jet have a similar direction. Due to the error of the secondary vertex measurement (finite detector resolution, ...), the decay length has a certain error  $\sigma(L_{XY})$ . The ratio  $L_{XY}/\sigma(L_{XY})$  describes the decay length significance and is denoted as  $S$ . A second variable is the invariant mass of the secondary vertices,  $M_{Sec.Vertex}$ . For the calculation of  $M_{Sec.Vertex}$  the pion mass is assumed for each track.



## 6. Secondary vertices from jets as reference axes

In previous analyses [1] secondary vertices associated to jets were used. Jets are collimated bundles of hadrons in the detector. They were reconstructed from energy flow objects combining track and calorimeter information using the  $k_T$  cluster algorithm. The reconstructed jets were selected for this study if they fulfill the selection cuts described below.

### 6.1. Jet selection

In this study only jets with a traverse energy  $E_T > 2.5\text{GeV}$  and  $-1.6 < |\eta| < 2.2$  were selected. The tracks fitted to a secondary vertex had to be well-reconstructed. The selection cuts for the tracks and vertices are summarised in the appendix in section A.2.

The previous analysis [1] selected the same jets apart from a higher  $E_T$  cut:  $E_T > 5.0\text{GeV}$ . In the following, these jets are referred to as *high  $E_T$  jets*, the jets with  $2.5\text{GeV} < E_T < 5.0\text{GeV}$  as *low  $E_T$  jets* and *all jets* means all jets with  $E_T > 2.5\text{GeV}$ .

### 6.2. Significance distributions from high $E_T$ jets

Using the decay length from the high  $E_T$  jets, the significance distribution shown in Fig.1 can be derived. The symmetric part (around 0) is caused by detector resolution effects. The asymmetric part originates from the long-lived particles containing  $b$  and  $c$  quarks. To determine the asymmetric part, one can mirror the left side of the significance distribution ( $S^-$ ,  $S < 0$ ) onto the right side ( $S^+$ ,  $S > 0$ ) and subtract them. This mirrored and subtracted significance distribution is denoted as  $S^+ - S^-$  in the following.

To extract the contributions from  $b$ ,  $c$  and *light flavor (LF)* in the data sample, a binned  $\chi^2$  fit of the  $S^+ - S^-$  distribution was performed in three different mass bins. A detailed description can be found in [1].

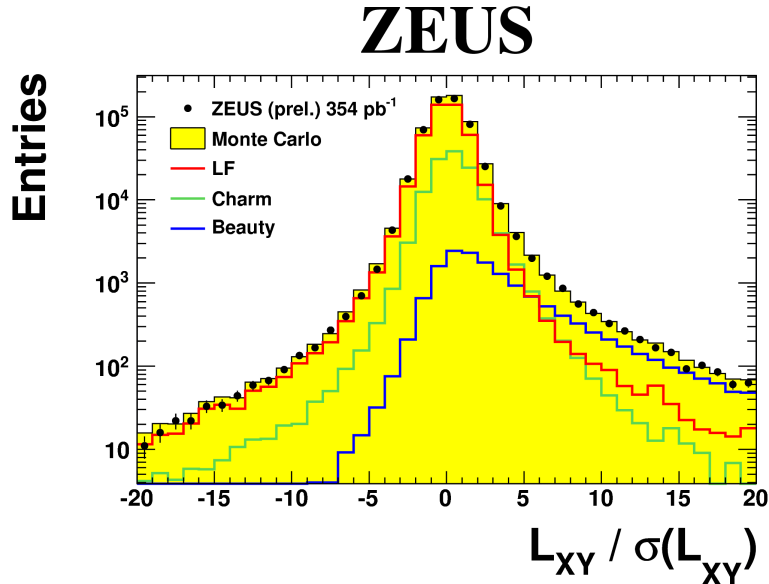


Figure 1: Significance distributions from high  $E_T$  jets, [1].

### 6.3. Comparison between high $E_T$ jets and all jets

One part of my project was to study the extension of the jet  $E_T$  range for secondary vertices. This has been done using  $b$  and  $c$  MC samples (cp. section 3). The significance and mirrored significance distributions for the  $b$  and  $c$  samples for high  $E_T$  jets and all jets are shown in Fig. 2.

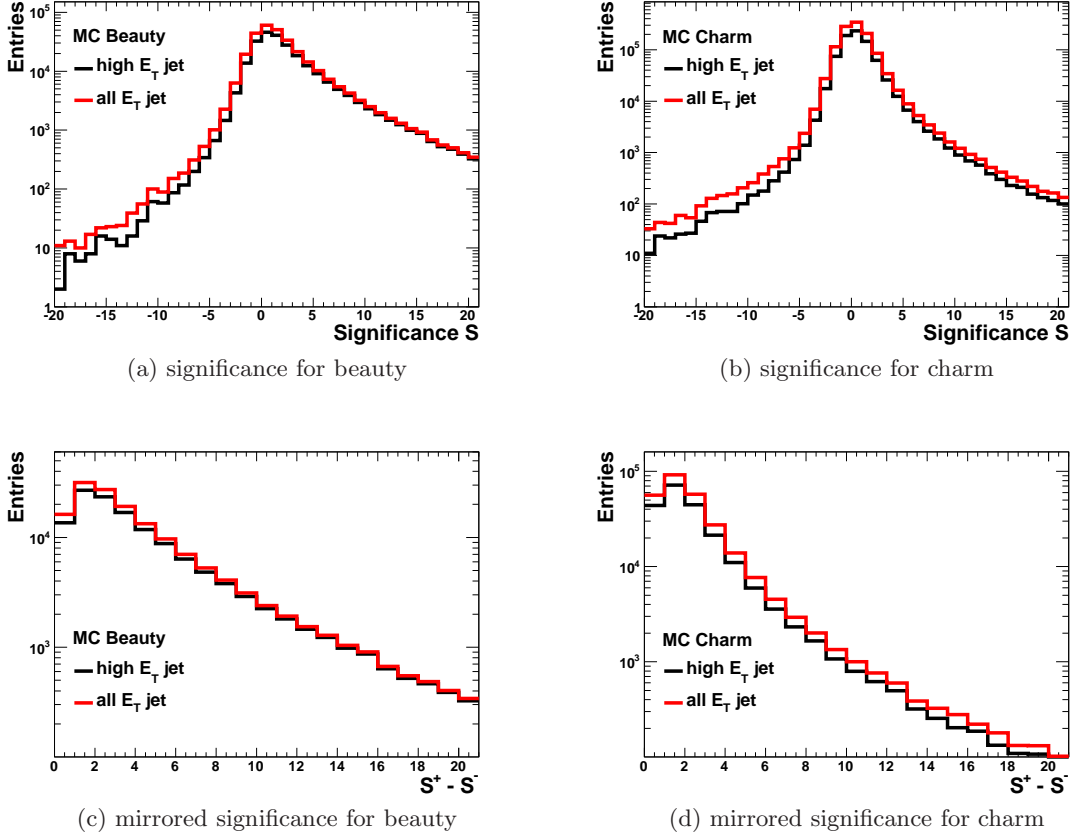


Figure 2: Significance and mirrored significance distributions for beauty and charm from high  $E_T$  jets (black) and all jets (red).

Most of the additional vertices for beauty are distributed almost symmetrically. The mirrored significance distributions show that the additional entries for the charm for the low  $E_T$  jets are more asymmetric than for the beauty.

This is expected since for low  $p_T$  the more massive  $b$ -hadrons ( $m_b \approx 4.75 \text{ GeV}$ ) tend to decay more isotropic in the detector than the  $c$ -hadrons ( $m_c \approx 1.5 \text{ GeV}$ ). Therefore, a low  $p_T$  charm quark is more likely to produce a collimated jet with  $E_T < 5 \text{ GeV}$  than a low  $p_T$  beauty quark.

## 7. Secondary vertices from Pseudo Thrust axes as reference axes

To get access to the low  $p_T$  region of produced heavy quarks, one part of my project was to study secondary vertices associated to pseudo thrust axes. The pseudo-thrust axes have originally been defined to separate heavy quarks produced near kinematic threshold from those giving rise to collimated di-jet systems. Heavy quark pairs produced close to their kinematic threshold have very low momenta and thus do not produce jets but rather a broad

spray of particles in the detector. The definition and a description of how the pseudo thrust is calculated is given in section 7.1. A few aspects of the implementation are described in section 7.2. The applied selection cuts for the pseudo thrust axes are given in section 7.3. In section 7.4 the usage of pseudo thrust axes and jets as reference axes for secondary vertices is compared and in section 7.6 a comparison between projecting onto jets and projecting onto pseudo thrust axes is done.

## 7.1. Pseudo Thrust

The pseudo thrust ( $T_{pseudo}$ ) is sensitive to the event shape and the definition is given by:

$$T_{pseudo} = \frac{\sum_{i=1}^{nZUFOS} \vec{p}_i \cdot \vec{T}_1 + \sum_{i=1}^{nZUFOS} \vec{p}_i \cdot \vec{T}_2}{\sum_{i=1}^{nZUFOS} |\vec{p}_i|}$$

The sums run over all reconstructed ZUFOS [7], where the  $\vec{p}_i$  are the corresponding momenta and the unit vectors  $\vec{T}_1$  and  $\vec{T}_2$ , called thrust axes in the following, are iterated until the scalar  $T_{pseudo}$  is maximised. The exact maximisation procedure for photoproduction can be found in [7]. For DIS it can be shortly summarised as follows:

- The pseudo thrust is maximised in the Breit frame analogue to [7]. The Breit frame is defined by  $2x\vec{p} + \vec{q} = 0$ , where  $x$  is the Bjorken scaling variable,  $\vec{p}$  the momentum of the proton and  $\vec{q}$  the momentum of the exchanged boson. A more detailed description can be found in [8].
- The thrust axes are iterated so that  $T_{pseudo}$  is maximized.
- After the maximisation the thrust axes are back-boosted to the lab frame.

Due to the back-boost of the thrust axes, there can be kinks in the  $\theta$  and  $\varphi$  plane. As an example, an analysed MC  $b\bar{b}$  event and the calculated pseudo thrust axes are shown in Fig. 3.

The value of  $T_{pseudo}$  is close to 1 for a perfectly back to back event with a very small spread and approaches 0.5 for isotropic events in the Breit frame.

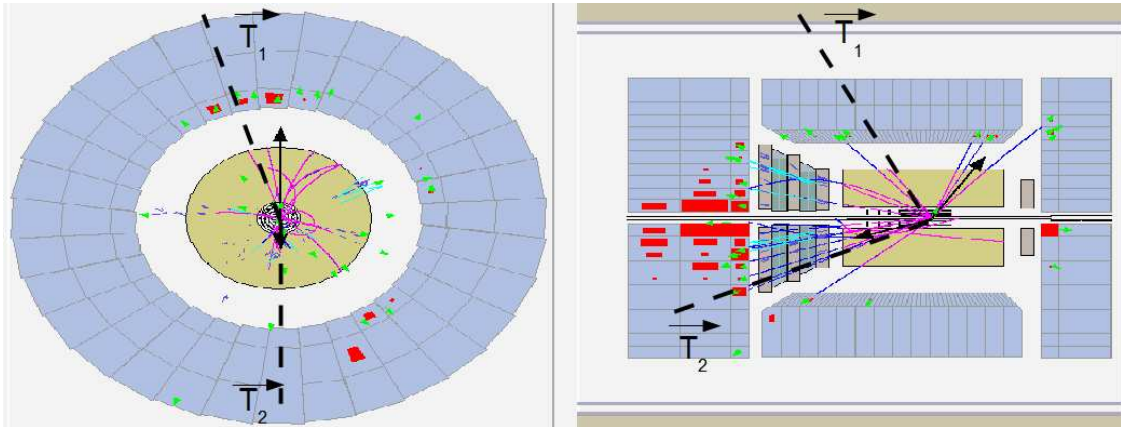


Figure 3: Event display of an analysed MC  $b\bar{b}$  event with the calculated pseudo thrust axes  $\vec{T}_1$  and  $\vec{T}_2$ .

## 7.2. Implementation of the pseudo thrust axes

For the calculation in the Breit frame, required for the calculation of the pseudo thrust axes, the proton remnant has to be removed. The proton remnant has been defined as all particles with  $\theta < 20^\circ$  in the lab frame.

Unfortunately, the algorithm calculating the pseudo thrust axes in the used Common Ntuples (v04b) has a bug in the back-boost so that the direction of the pseudo thrust axes is slightly changed. But this bug is found to only slightly affect the results of this study. Furthermore, the correct pseudo thrust axes should work even better for my kind of studies than the used slightly buggy ones.

## 7.3. Pseudo thrust cuts

The selection cuts for the pseudo thrust axes are similar to the cuts applied to the jets. In this study only thrust axes with  $-1.6 < |\eta| < 2.2$  were used. The secondary vertex associated to a pseudo thrust axis also has to satisfy the same criteria as for jets. The summarised selection cuts can be found in the appendix in section A.3.

## 7.4. Comparison between high $E_T$ jets and pseudo thrust axes

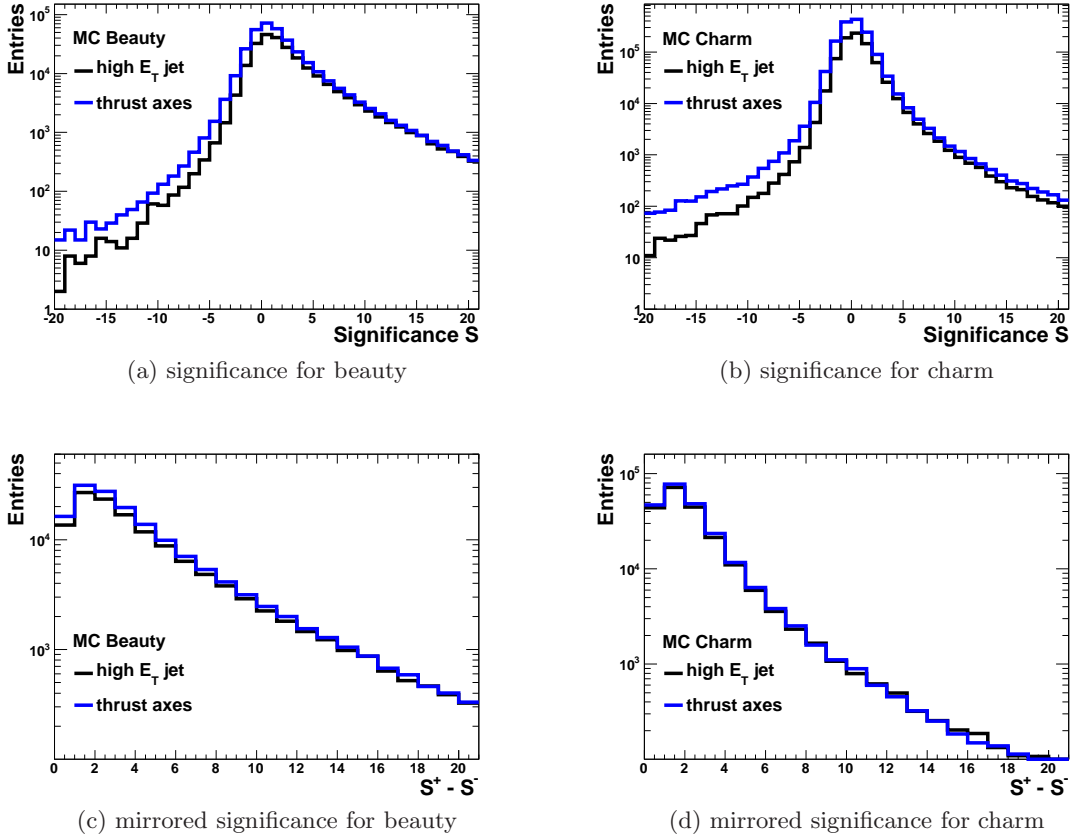


Figure 4: Significance and mirrored significance distributions for beauty and charm from high  $E_T$  jets (black) and pseudo thrust axes (blue).

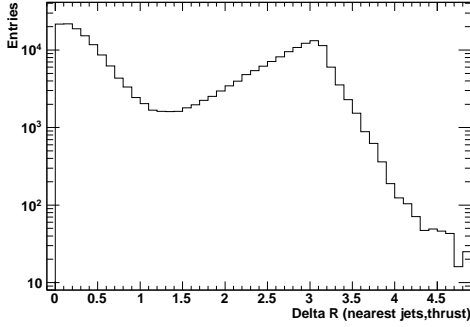


For the comparison between the usage of high  $E_T$  jets and pseudo thrust axes for secondary vertexing the  $b$  and  $c$  MC samples (cp. section 3) have been used. The significance and mirrored significance distributions for  $b$  and  $c$  from high  $E_T$  jets and pseudo thrust axes as reference axes are shown in Fig. 4.

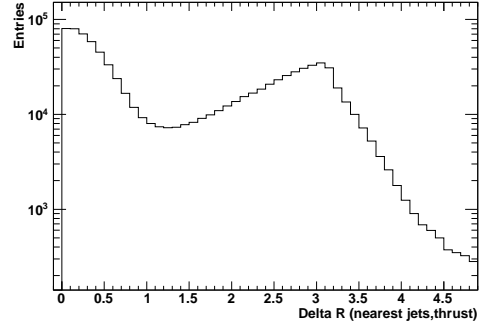
More secondary vertices can be found for pseudo thrust axes compared to jets as reference axes. The mirrored significance distributions show that the usage of pseudo thrust axes and jets have similar performance for the asymmetric part. Therefore, the usage of pseudo thrust axes for secondary vertices is reasonable.

### 7.5. Comparison between the direction of the pseudo thrust and the nearest jet

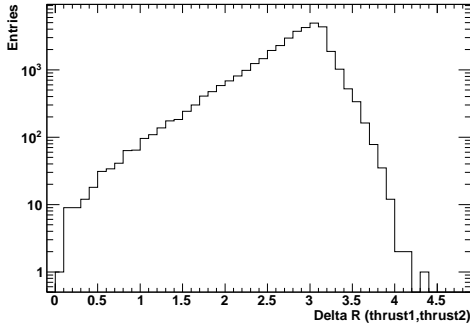
For a second comparison between the pseudo thrust and the jets, the direction of each is studied. For this aim the direction of the pseudo thrust axes and the nearest jet is compared if a secondary vertex with both reference axes types was found. The distance  $\Delta R = \sqrt{(\Delta\eta)^2 + (\Delta\varphi)^2}$  between the pseudo thrust axis and the nearest jet is shown in Fig. 5a and 5b. The distance  $\Delta R$  between both pseudo thrust axes if secondary vertices are found associated to both pseudo thrust axes is shown in Fig. 5c and 5d.



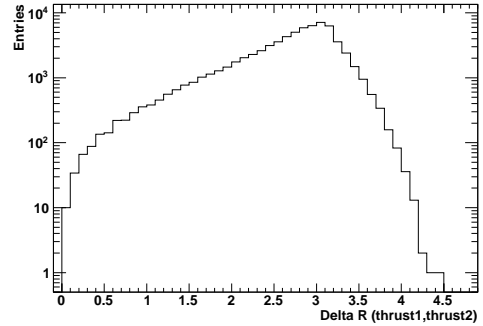
(a)  $\Delta R$  between pseudo thrust axes and nearest jet for beauty



(b)  $\Delta R$  between pseudo thrust axes and nearest jet for charm



(c)  $\Delta R$  between both pseudo thrust axes for beauty



(d)  $\Delta R$  between both pseudo thrust axes for charm

Figure 5: The distance  $\Delta R$  between pseudo thrust axes and nearest jet for beauty (a) and charm (b) and the distance  $\Delta R$  between both pseudo thrust axes for beauty (c) and charm (d) if a secondary vertex is associated to each of these reference axes.

As one can see from the  $\Delta R$  distributions for the beauty and charm MC sample in Fig. 5a and 5b most of the jets and pseudo thrust axes associated to a secondary vertex have a

similar direction ( $\Delta R < 1$ ) or an opposite direction ( $\Delta R \approx 3$ ).

The bump at  $\Delta R \approx 3$  can be understood with the  $\Delta R$  distributions for the beauty and charm MC sample in Fig. 5c and 5d. In most of the events where both pseudo thrust axes are associated to a secondary vertex, the direction of the pseudo thrust axes is back-to-back ( $\Delta R \approx 3$ ). The bump at  $\Delta R \approx 3$  is caused by events where both pseudo thrust axes are associated to a secondary vertex but only one jet associated to a secondary vertex is found or vice versa.

### 7.6. Comparison between projecting onto jets and onto pseudo thrust axes

To compare the performance of projecting onto the jet axis with the performance of projecting onto the pseudo thrust axes, events where one of the pseudo thrust axes and one jet have a similar direction,  $\Delta R < 1$ , have been selected. The comparison was done for high  $E_T$  jets and low  $E_T$  jets separately and the nearest jet in  $\eta$ - $\varphi$  space was always selected. The mirrored significance distributions for the  $b$  and  $c$  MC sample (cp. section 3) from these high  $E_T$ , all  $E_T$  jets and pseudo thrust axes are shown in Fig. 6.

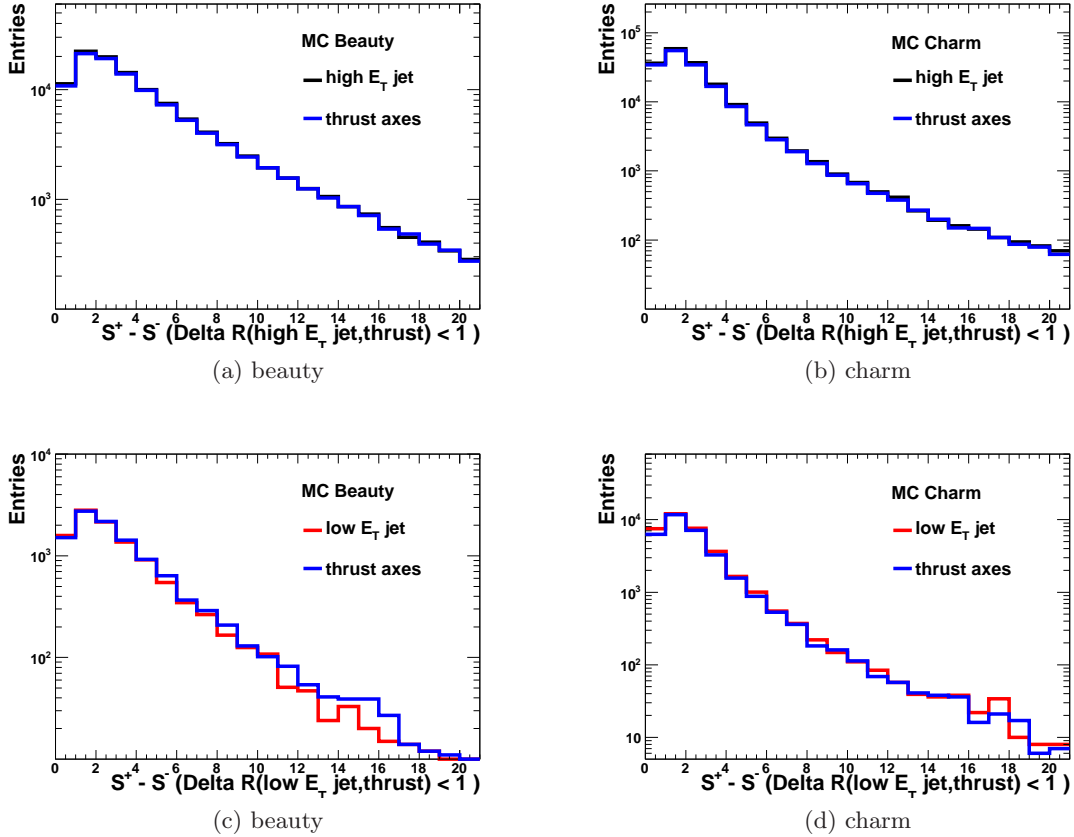


Figure 6: Mirrored significance distributions for beauty and charm from high  $E_T$  jets (black), low  $E_T$  jets (red) and pseudo thrust axes (blue) in events where the pseudo thrust and the jet have a similar direction,  $\Delta R < 1$ .

The mirrored significance distributions show that the usage of pseudo thrust axes and jets have similar performance. Therefore, the usage of pseudo thrust axes for secondary vertices is reasonable.

## 8. Secondary vertices from a combined method of jets and pseudo thrust axes

As one can see from section 6 and 7, the low  $E_T$  jets as well as the pseudo thrust axes are reasonable reference axes for secondary vertices. Since not all jet axes find the same secondary vertices as the pseudo thrust axes and vice versa it is promising to combine both methods. The combined method contains the secondary vertices associated to all jets and in addition the secondary vertices associated to the pseudo thrust axes if no jet within  $\Delta R < 1$  is present.

### 8.1. Comparison between combined method and the single methods

The combined method has been compared with all single methods using  $b$  and  $c$  MC samples (cp. section 3). The significance and mirrored significance distributions for  $b$  and  $c$  from the combined method, the pseudo thrust axes, all  $E_T$  jets and high  $E_T$  jets are shown in Fig. 7 for beauty and in Fig. 8 for charm.

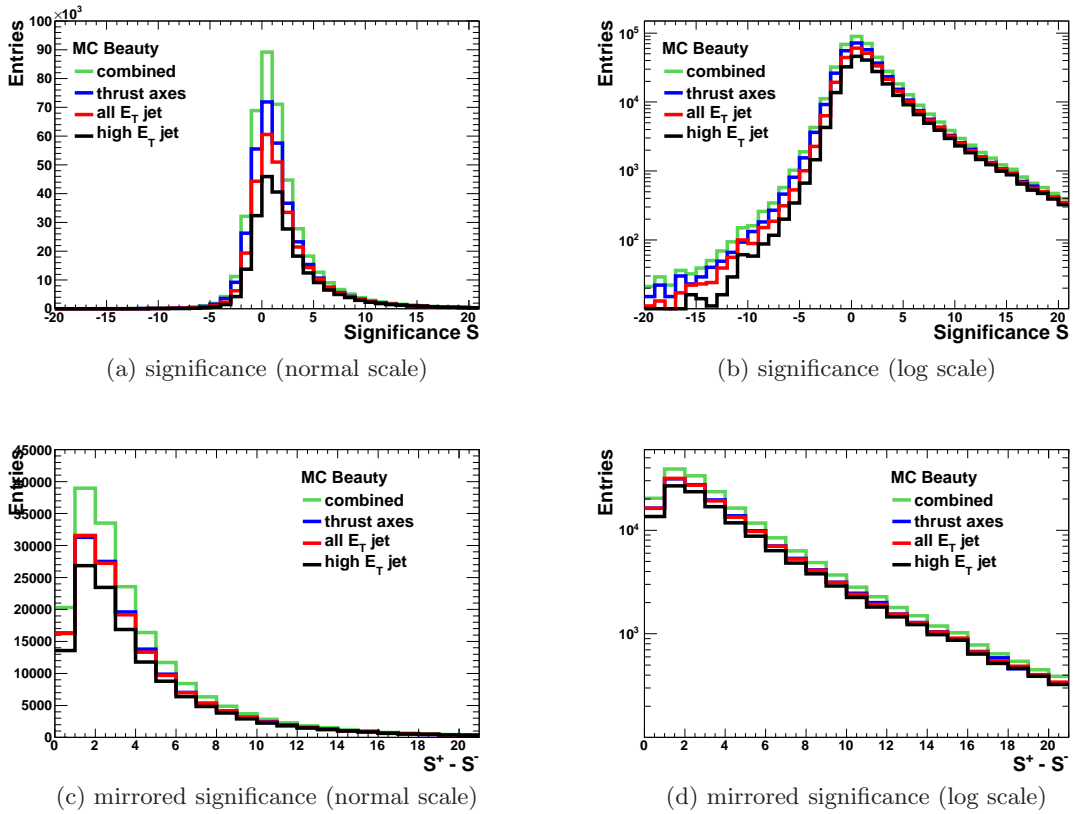


Figure 7: Significance and mirrored significance distributions for beauty from combined method (green), pseudo thrust axes (blue), all  $E_T$  jets (red) and high  $E_T$  jets (black).

As one can see from the significance distributions for the beauty MC sample in Fig. 7, the extension of the  $E_T$  range for the jets as well as the pseudo thrust as new reference axes enhance the statistics. But the combined method leads to the biggest improvement. The mirrored significance distribution shows that the gain in asymmetric events is substantial in each significance bin.

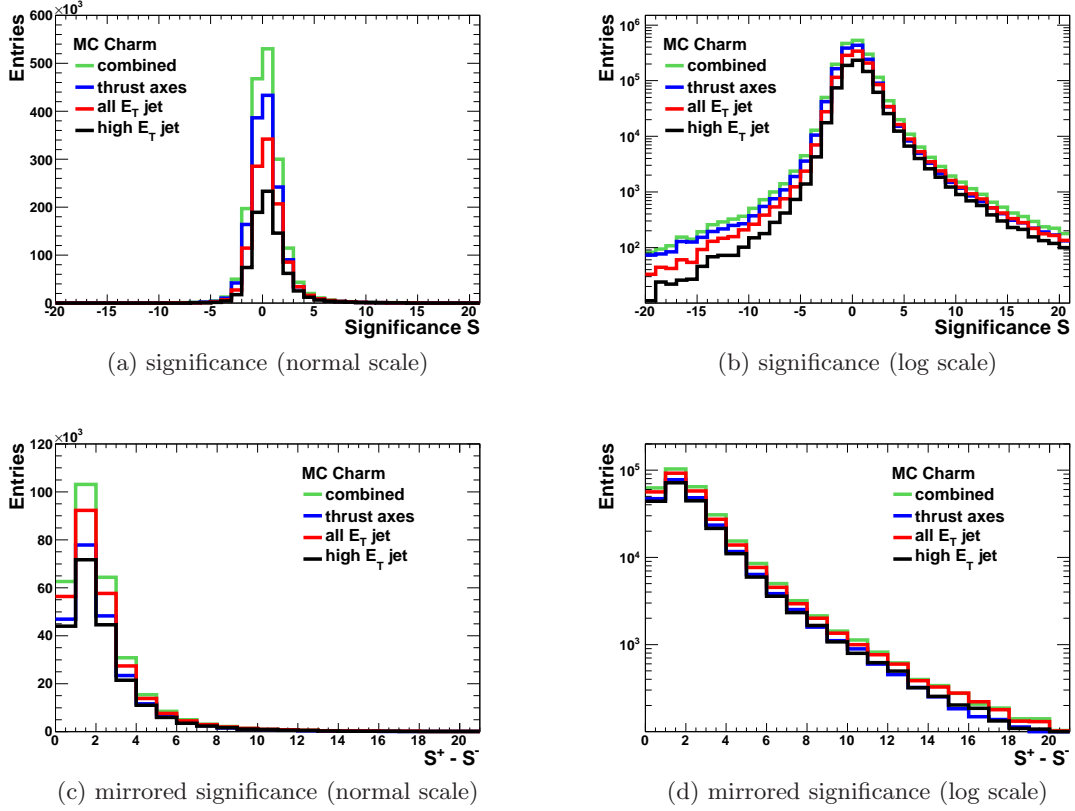


Figure 8: Significance and mirrored significance distributions for charm from combined method (green), pseudo thrust axes (blue), all  $E_T$  jets (red) and high  $E_T$  jets (black).

The significance distribution for the charm MC sample in Fig. 8 shows that the combined method enhances the statistics with respect to the single methods. But the comparison of the mirrored significances indicates that the combined method is an improvement with respect to the extension of the  $E_T$  range for the jets mostly at low significance bins.

## 9. The axis of the hadronic system for secondary vertices

In addition to the pseudo thrust axes as reference axes for secondary vertices also the axis of the hadronic system has been studied.

The hadronic system is given by the sum of every particle in the detector apart from the scattered electron. Unfortunately, the proton remnant was not in this case removed so that the direction of the hadronic system almost always points in the proton direction. The  $\eta$  distribution of the hadronic system in the MC  $b$  sample can be seen in Fig. 9. Thus the hadronic system as reference axis for secondary vertices has not been studied further.

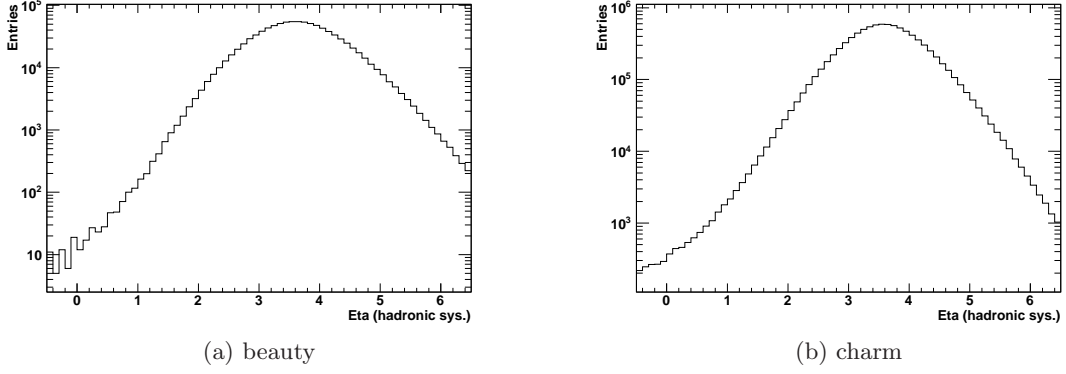


Figure 9: Eta ( $\eta$ ) distribution of the hadronic system after DIS event selection cuts for the beauty and charm MC sample.

## 10. Summary and Outlook

In my Summer Student project an extension the  $E_T$  range for jets and the usage of pseudo thrust axes for reconstruction of secondary vertices have been tested. It has been shown that both methods can increase the statistics for beauty and charm in the low  $E_T$  region. For beauty a combined method of jets and pseudo thrust axes for reconstructing secondary vertices increases the statistics most. For charm the extension of the  $E_T$  range is most effective in increasing the statistics and the combined method improves the statistics only slightly. The next step for this study is to test the new significance distributions in a further analysis similar to the one in [1]. Furthermore, the pseudo thrust value  $T_{pseudo}$  should be restudied when a correct pseudo thrust algorithm is been used for the next generation of the Common Ntuples.

## 11. Acknowledgements

I would like to thank my supervisor Achim Geiser, as well as Philipp Roloff, who helped me a lot.

## References

- [1] ZEUS Coll., ZEUS-Prel-10-004, 2010.
- [2] D.H. Perkins, *Introduction to High Energy Physics*, 4th edition, Cambridge University Press, Cambridge, UK, 2010.
- [3] ZEUS Coll. S. Chekanov et al., Phys Lett. **B 599**, 173, 2004;  
H1 Coll., A. Aktas et al., Eur. Phys. J. **C 41**, 453, 2005.
- [4] ZEUS Coll. H. Abramowicz et al., DESY-10-047, 2010.
- [5] C. Amsler et al. *Review of particle physics*. Phys. Lett. **B667:1**, 2008.
- [6] V. E. Schönberg, *Measurement of beauty and charm photoproduction using inclusive secondary vertexing with the ZEUS detector at HERA*, Ph.D thesis, Bonn, Germany, Bonn-IR-2010-05, 2010.
- [7] I. Bloch, *Measurement of Beauty Production from Dimuon Events at HERA/ZEUS*, Ph.D thesis, Hamburg, Germany, DESY-THESIS-2005-034, DESY, 2005.
- [8] T. Kluge, *Measurement and QCD Analysis of Event Shape Variables in Deep-Inelastic Electron-Proton Collisions at HERA*, Ph.D thesis, Hamburg, Germany, DESY-THESIS-2004-024, DESY, 2004.

# Appendix

## A. Applied Cuts

### A.1. Event selection cuts

To select DIS events in the range  $5 \text{ GeV}^2 < Q^2 < 1000 \text{ GeV}^2$  and  $0.02 < y < 0.7$  the SPP09 OR HLF17 OR HPP31 trigger was used and the following cuts have been applied:

- Sinistra probability  $> 0.9$
- $E'_e > 10.0 \text{ GeV}$
- $y_{JB} > 0.02$
- $y_e < 0.7$
- $44.0 \text{ GeV} < E - P_z \text{ (ZUFOS)} < 65.0 \text{ GeV}$
- $|X_e| > 13 \text{ cm}$  OR  $|Y_e| > 13 \text{ cm}$
- $5.0 \text{ GeV}^2 < Q_{DA}^2 < 1000.0 \text{ GeV}^2$
- $Z_{Prim.Vertex} < 30 \text{ cm}$

The used cuts are the same used in similar kind of analyses.

## A.2. Jet selection cuts

In this study the following jet selection cuts have been applied:

- $-1.6 < \eta < 2.2$
- $E_T > 5.0 \text{ GeV}$  for high  $E_T$  jets
- $E_T > 2.5 \text{ GeV}$  for all jets
- $2.5 \text{ GeV} < E_T < 5.0 \text{ GeV}$  for low  $E_T$  jets

### A.2.1. Tracks for secondary vertexing selection cuts

In this study the following selection cuts for tracks for the secondary vertices from jets have been applied:

- ZTT tracks with  $p_T > 0.5 \text{ GeV}$
- Number of MVD hits  $\geq 4$
- Distance to closest jet  $R = \sqrt{(\Delta\eta)^2 + (\Delta\phi)^2} < 1$

The used cuts are the same used in similar kind of analyses.

### A.2.2. Secondary vertex from jets selection cuts

In this study the following selection cuts for the secondary vertices from jets have been applied:

- $|Z_{Sec.Vertex}| < 30 \text{ cm}$
- Distance  $BS - Sec. Vertex < 1 \text{ cm}$  (in  $X - Y$  plane)
- $\chi^2/ndf < 6$  (from secondary vertex fit)
- $1.0 \text{ GeV} < M_{Sec.Vertex} < 6.0 \text{ GeV}$

The used cuts are the same used in similar kind of analyses.

## A.3. Pseudo thrust selection cuts

In this study the following pseudo thrust selection cuts have been applied:

- $-1.6 < \eta < 2.2$

### A.3.1. Secondary vertex from pseudo thrust selection cuts

In this study the following selection cuts for the secondary vertices from pseudo thrust have been applied:

- $|Z_{Sec.Vertex}| < 30 \text{ cm}$
- Distance  $BS - Sec. Vertex < 1 \text{ cm}$  (in  $X - Y$  plane)
- $\chi^2/ndf < 6$  (from secondary vertex fit)
- $1.0 \text{ GeV} < M_{Sec.Vertex} < 6.0 \text{ GeV}$